PNNL-16942

Pacific Northwest
National Laboratory
Operated by Battelle for the
U.S. Department of Energy

Laser Remote Sensing: FY07 Summary Report

WW Harper
JD Strasburg
EC Golovich
JS Thompson
TL Stewart
MT Batdorf
A Mendoza

September 2007

Prepared for the U.S. Department of Energy
under Contract DE-AC05-76RL01830

DISCLAIMER

PACIFIC NORTHWEST NATIONAL LABORATORY
operated by
BATTELLE
for the
UNITED STATES DEPARTMENT OF ENERGY
under Contract DE-AC05-76RL01830

Printed in the United States of America

Available to DOE and DOE contractors from the
Office of Scientific and Technical Information,
P.O. Box 62, Oak Ridge, TN 37831-0062;
ph: (865) 576-8401
fax: (865) 576-5728
email: reports@adonis.osti.gov

Available to the public from the National Technical Information Service,
U.S. Department of Commerce, 5285 Port Royal Rd., Springfield, VA 22161
ph: (800) 553-6847
fax: (703) 605-6900
email: orders@ntis.fedworld.gov
online ordering: http://www.ntis.gov/ordering.htm


This document was printed on recycled paper.
(9/2003)

PNNL-16942

Laser Remote Sensing: FY07 Summary Report

W. W. Harper
J. D. Strasburg
E. C. Golovich
J. S. Thompson
T. L. Stewart
M. T. Batdorf
A. Mendoza

September 2007

Prepared for
the U.S. Department of Energy
under Contract DE-AC05-76RL01830

Pacific Northwest National Laboratory
Richland, Washington 99352

Summary

Standoff detection and characterization of chemical plumes using Frequency Modulated Differential Absorption LIDAR (FM-DIAL) is a promising technique for the detection of nuclear proliferation activities. For the last several years Pacific Northwest National Laboratory (PNNL) has been developing an FM-DIAL–based remote sensing system as part of PNNL's Infrared Sensors project within NA-22's Enabling Technologies portfolio. In FY06 the remote sensing effort became a stand-alone project within the Plutonium Production portfolio with the primary goal of transitioning technology from the laboratory to the user community.

Current systems remotely detect trace chemicals in the atmosphere over path lengths of hundreds of meters for monostatic operation (without a retro-reflector target) and up to ten kilometers for bistatic operation (with a retro-reflector target). The FM-DIAL sensor is sensitive and highly selective for chemicals with narrowband absorption features on the order of 1–2 cm^{-1}; as a result, the FM-DIAL sensors are best suited to simple di-atomic or tri-atomic molecules and other molecules with unusually narrow absorption features. A broadband sensor is currently being developed. It is designed to detect chemicals with spectral features on the order of several 10s of wavenumbers wide. This will expand the applicability of this technology to the detection of more complicated molecules. Our efforts in FY07 focused on the detection of chemicals associated with the PUREX process.

The highest value performance measure for FY07, namely the demonstration of the Broadband Laser Spectrometer (BLS) during chemical release experiments, was successfully achieved in June, July, and August of this year. Significant advancements have been made with each of the other tasks as well. A short-wave infrared version of the miniature FM-DIAL (FM-Mini) instrument was successfully demonstrated during field tests in June. During FY07 another version of the FM-Mini was built using long-wave infrared components. This instrument was deployed for field tests in July and August. The modeling task continued to study the impact of speckle on the FM-DIAL system as well as make further advancements in the sophistication of the numerical simulations.

Acronyms

BLS	Broadband Laser Spectrometer
DFB	distributed feedback
FM-DIAL	Frequency Modulated Differential Absorption LIDAR
FM-Mini	miniature FM-DIAL
FP	Fabry-Perot
HTS	Hanford Town Site
LIDAR	light detection and ranging
LWIR	long-wave infrared
NTS	Nevada Test Site
PNNL	Pacific Northwest National Laboratory
PPG	portable plume generator
QCL	quantum cascade lasers
SNR	signal-to-noise ratio
SWIR	short-wave infrared
TCC	Test Cell C

Contents

Figures

Tables

1.0 Introduction

Standoff detection and characterization of chemical plumes using Frequency Modulated Differential Absorption LIDAR (FM-DIAL) is a promising technique for the detection of nuclear proliferation activities. For the last several years Pacific Northwest National Laboratory (PNNL) has been developing an FM-DIAL–based remote sensing system as part of PNNL's Infrared Sensors project within NA-22's Enabling Technologies portfolio. In FY06, the remote sensing effort became a stand-alone project within the Plutonium Production portfolio with the primary goal of transitioning technology from the laboratory to the user community.

During the last five years, the trailer-based FM-DIAL sensor has been deployed in over two dozen field campaigns in a variety of meteorological conditions. Several field experiments occurred in the high-desert environment of the Hanford Site in eastern Washington. The system has also been deployed in a maritime environment at PNNL's Marine Sciences Research Laboratory in Sequim, Washington, as well as the desert environment of the Nevada Test Site (NTS). The FM-DIAL sensor has successfully detected multiple chemicals in real-world plume release experiments, including the Shrike and Tarantula tests at NTS. Patents have been submitted on the intensity normalization techniques developed to mitigate the effects of atmospheric turbulence as well as the broadband detection techniques. In addition, the trailer-based FM-DIAL technology has been funded by and demonstrated for a specific user.

Current systems remotely detect trace chemicals in the atmosphere over path lengths of hundreds of meters for monostatic operation (without a retro-reflector target) and up to ten kilometers for bistatic operation (with a retro-reflector target). The FM-DIAL sensor is sensitive and highly selective for chemicals with narrowband absorption features on the order of 1–2 cm^{-1}; as a result, the FM-DIAL sensors are best suited to simple di-atomic or tri-atomic molecules and other molecules with unusually narrow absorption features. A broadband sensor is currently being developed. It is designed to detect chemicals with spectral features on the order of 10s of wavenumbers wide. This will expand the applicability of this technology to the detection of more complicated molecules. Both narrowband and broadband sensors have the potential for isotopic detection of low-Z elements; for example, detecting the presence of heavy water in the atmosphere. In general, the remote sensing systems are conducive to fence-line or surface-at-a-distance monitoring. In addition, the miniaturized system, which is also being developed as part of this effort, could be mounted on a moving platform. Our efforts in FY07 focused on the detection of effluents associated with the PUREX process. The two high-value, mission-relevant chemicals discussed in this report have the codenames *Michigan* and *New Hampshire*.

1.1 Project Organization

The remote sensing project was organized into four major tasks and two minor tasks:

- ***FM-DIAL Miniaturization***: Design, construct, and test a long-wave infrared FM-DIAL sensor for rapid deployment, remote control, and autonomous operation in harsh environmental conditions.

- ***Broadband Laser Spectrometer***: Continue to address the technical challenges associated with a broadband sensor.

- ***Modeling***: Continue development of numerical simulations and models of sensor performance. Potential areas of development include the effects of moving platforms or moving targets and the variability of atmospheric constituents.

- ***NTS Process Simulation***: Participate in the NTS Process Simulation experiments as part of the Tarantula program. Deploy two different remote sensors during the Process Simulation.

Two minor tasks focused on procuring new quantum cascade lasers (QCLs) from Maxion Technologies and optimizing the narrowband and broadband sensors for monostatic performance.

1.2 Proposed FY07 Milestones

The highest value performance measure for FY07 was the demonstration of the broadband sensor during chemical release experiments. Other milestones and deliverables included in the statement of work were

- FM-DIAL Miniaturization
    - Miniaturization of narrowband FM DIAL sensor using LWIR components
    - Demonstration of 10 km bistatic operation
- Broadband Laser Spectrometer
    - Field experiments using chemicals related to spent nuclear fuel processing conducted at Hanford site
- NTS Process Simulation
    - Participation in NTS Process Simulation

1.3 FY07 Accomplishments

The highest value performance measure for FY07, namely the demonstration of the Broadband Laser Spectrometer (BLS) during chemical release experiments, was successfully achieved in June, July, and August of this year. In early FY07, the BLS was transitioned from the laboratory to a trailer-based platform in order to facilitate additional field studies. A preliminary set of field tests took place in December and the results were encouraging. The BLS was optimized for the detection of *Michigan* for the June field campaign at the Hanford Town Site. Following the first successful set of chemical release experiments, the laser was switched out for one optimized for the detection of *New Hampshire*. This laser was used for the July releases at the Hanford Town Site as well as the August Brown Recluse Tests at the Nevada Test Site.

Significant advancements have been made with each of the other tasks as well. The short-wave infrared (SWIR) FM-Mini successfully participated in the June chemical releases of *Michigan*. A second version of the FM-Mini sensor was integrated with long-wave infrared (LWIR) components and was deployed for the July *New Hampshire* releases and the August Brown Recluse Tests.

The Modeling task continued to study the effects of speckle on the FM-DIAL system. Although speckle is not a large noise source when using retro-reflector targets, it is critical when considering the return signal from a diffuse reflectance target. Advances were also made with the numerical simulations to include tip/tilt and beam wander effects as well as moving phase screens that allow us to explore the temporal effects of turbulence. Finally, we have started to consider alternative approaches to deal with the scale problem in the simulations.

During FY07, we did not purchase new quantum cascade lasers from Maxion. A broadband, Fabry-Perot (FP) QCL for the BLS was delivered at the end of FY06. This laser was designed to detect *Michigan* and fulfilled requirements necessary for FY07 plans. In FY05, a narrowband, distributed feedback (DFB) QCL and an FP QCL were purchased for the detection of *New Hampshire*. These lasers were used in the BLS and FM-Mini sensors. We are planning to procure additional QCLs in early FY08 and are working with subject matter experts to determine what wavelength region to target.

Initial work went into considering how to design for 1-km monostatic operation and the results were not encouraging. Given the power available from current SWIR and LWIR devices, achieving reasonable results from diffuse scattering at 1 km does not look promising. One of our proposed deliverables for FY08 was demonstration of 1-km monostatic performance with both the FM-Mini and the BLS. Because of the difficulty in achieving reasonable diffuse scattering results, we are anticipating a re-scope of our FY08 life cycle plan.

2.0 FM-DIAL Miniaturization

In FY06, PNNL miniaturized the narrow-band FM-DIAL sensor system to create an autonomous, remotely controlled, field-deployable system operating in the short-wave infrared. Similar to the trailer-based sensor, the miniature system, known as FM-Mini, is operated in a bi-static arrangement, using a retro-reflector to boost return signal intensity. In FY07, the FM-Mini was modified to operate in the long-wave infrared using quantum cascade lasers.

The FM-Mini system was designed to be considerably more compact than the previous trailer-based FM-DIAL sensor. Figure 2.1 depicts the experimental layout of the LWIR FM-Mini system. The main laser source is a cryogenically cooled LWIR QC laser. A portion of the beam is split off and sent to a reference cell filled with the chemical of interest. The remaining part of the beam is sent to exit the enclosure. The beam divergence of the QC lasers is 1 mrad.

The optical components are attached to a 600-mm × 600-mm × 25-mm breadboard housed in a 24-in. × 24-in. × 16-in. enclosure, as shown in Figure 2.2. The new LWIR optics enclosure is slightly larger than the SWIR optics enclosure to accommodate the liquid nitrogen Dewar that houses the QC laser. The optics enclosure is mounted on a Gimbal mount to allow for directionality.

Minimal electronics are necessary to run the FM-Mini system. A laser control box, laser power supply, lock-in amplifier, computer, and a data acquisition card are the only necessary components that are housed in a transportable crate. Figure 2.3 shows the inside of the electronics crate. For comparison, the trailer-based FM-DIAL sensor occupied a 3-ft × 6-ft optical bench and required two crates of electronics.

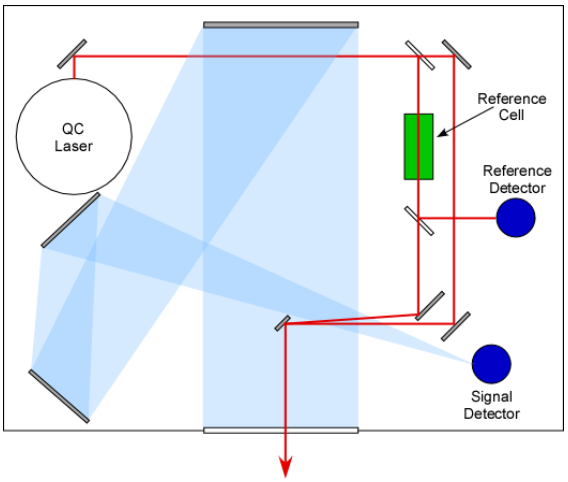

Figure 2.1. Schematic of the Optical Layout of the LWIR FM-Mini System

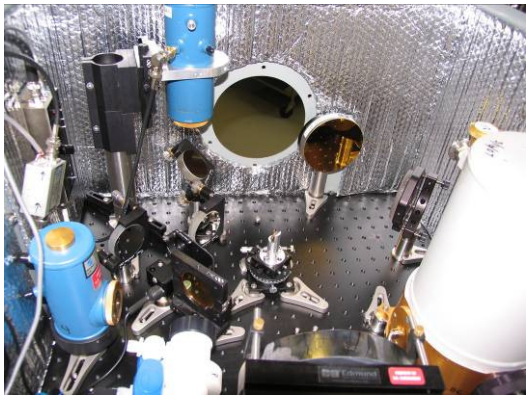

Figure 2.2. Layout of the LWIR FM-Mini Optics

Figure 2.3. Power Supply, Current Controller, Lock-In Amplifier and Computer Required to Run the System

In order to keep the electronics working at acceptable operating temperatures, a small air conditioner was also housed in the lower portion of the electronics crate. As shown in Figure 2.4, duct tubing was run from the electronics crate to the optics box; one for cold air to be sent to the optics box and the other for warm air return from the optics box to the crate. To keep solar heating of the system at a minimum, the electronics crate was painted a light-sand color, insulation was placed along the walls of the optics box, and reflective insulation was placed on the top of the optics box.

Figure 2.4. FM-Mini System Deployed in the Field

3.0 Broadband Laser Spectrometer

In FY07, we transitioned the BLS from the laboratory to a trailer-based platform that allows the opportunity to deploy the system to any location. The trailer contains the resources necessary to successfully deploy at locations at the Hanford Town Site (HTS), as well as longer trips to the Nevada Test Site. This year we deployed to HTS three times and to NTS for the process simulation tests. In each of the tests that we participated, we have had very successful results with the BLS. Looking at the data for the whole year, we observed a positive detection every time the target chemicals were released. The field testing resulted in an excellent data source to show the utility, sensitivity, and potential limitations of the technique.

Our target chemicals this year were the mission-relevant molecules code named *Michigan* and *New Hampshire.* From our previous work, we already had DFB QCLs to detect *New Hampshire*. We also had devices fabricated in FY06 specifically for *Michigan* detection. These devices were received late in the fiscal year, and were tested in FY07. We also did some preliminary tests this year using an on-hand DFB device for methanol detection. As the broadband technique was not field-tested before this year, we quickly transitioned the system to the trailer. Figure 3.1 shows the BLS installed in the trailer-based platform. Preliminary field tests took place during the first quarter. These tests gave confidence in our approach and guidance for refining the system in order to achieve this year's deliverables.

We were successful in executing our highest value deliverable for FY07 in the third quarter – detection of *Michigan* with the broadband system at HTS. In the fourth quarter we were successful in detecting *New Hampshire* at HTS and NTS.

Figure 3.1. Broadband Laser Spectrometer Installed in the Trailer

3.1 Reconfiguring the System to Detect *New Hampshire*

After the successful *Michigan* field tests in June, we reconfigured the broadband system for detection of *New Hampshire*. This involved changing the laser to a different target wavelength, and adjusting the wavelength dispersion optics (monochromator). *New Hampshire* does not have broadband features but rather a multitude of sharp absorption features with maximum widths of about 0.1 cm^{-1}. The BLS was developed to detect broadband chemical features ranging from several wavenumbers up to about 30 cm^{-1}; however, the system is quite versatile and it is possible to use it to detect narrowband features. There are some tradeoffs because detecting narrowband features is not what the system was designed for; as a result, there is some sensitivity degradation when applying it toward narrow features. We made some enhancements to the monochromator to minimize loss of sensitivity. While it is not optimal to detect narrowband features with the broadband sensor, we were quite successful in detecting the released quantities of *New Hampshire*.

A trace of representative data is shown in Figure 3.2 where reference (no signature) and signal (with signature) is overlaid at the top of the graph. The data shows the characteristic partially resolved laser modes that are emitted from the QC laser. Notice that at 1047 cm^{-1}, a single mode is reduced in intensity due to absorption of a chemical plume. In typical broadband data, multiple modes would be attenuated. The PNNL database spectrum is plotted in black for reference. The key signature overlaps well with our calculated absorbance spectrum. The smaller features do not show up in our spectrum because of the way that the broadband technique is used to look for narrow features. The emitted laser modes are high-resolution and are spaced at 0.65 cm^{-1}, with no power between modes. Unless the other features are an integral multiple of modes from the main feature, they will be missed and therefore not detected. We chose to optimize the system for the largest absorption feature centered near 1046 cm^{-1}.

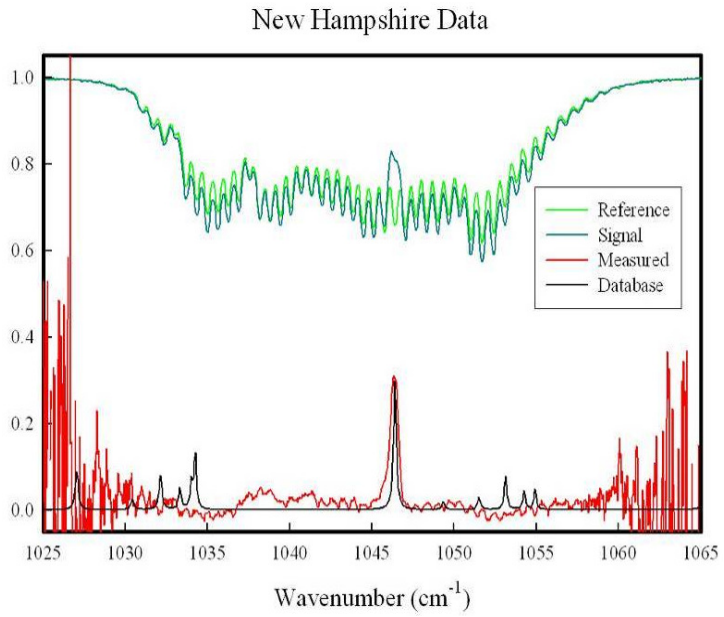

Figure 3.2. Representative Data Showing the Raw BLS Data and the Processed *New Hampshire* Absorption Spectra

4.0 Modeling Development

4.1 Impact of Speckle on the FM-DIAL System

Laser speckle is the coherent interference pattern produced at the receiving aperture of a light detection and ranging (LIDAR) system when the target is rough at the scale of the laser's wavelength. The rough surface randomly scatters the signal, which is then diffracted as it travels to the receiving telescope. The resulting intensity at the telescope has a granular appearance, as can be seen in Figure 4.1, and represents a significant source of noise to the LIDAR system.

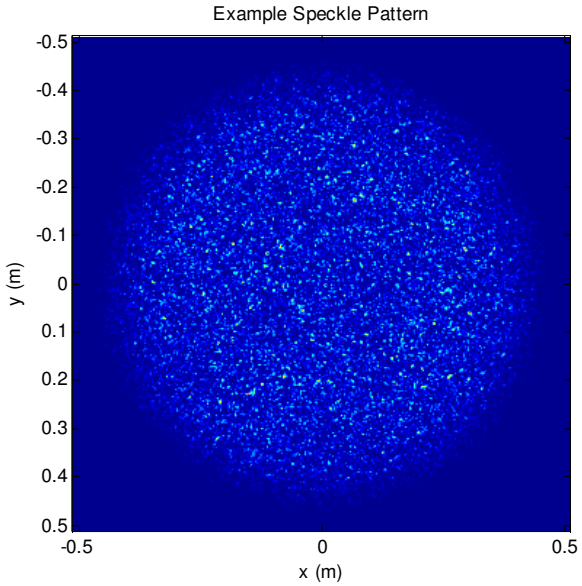

Figure 4.1. Example Speckle Pattern

Interestingly, the noise introduced by speckle is independent of the target surface characteristics. Instead, the noise only depends on the spatial characteristics of the signal at the target surface and on the geometry of the receiving telescope's aperture. Further, if these geometries can be written in an analytic form, the statistics of the speckle pattern can be calculated without resorting to Monte-Carlo simulations. Otherwise, simulations can be run for general geometries in order to accumulate data for the statistics.

During FY07 the speckle problem and its potential impact on the FM-DIAL system was revisited. A preliminary analysis was conducted in FY00 by D. M. Sheen[(a)] before an actual FM-DIAL system had been built. He based much of his analysis on work by Abarbanel et al. (1994), which reviewed the issues involved with using LIDAR for remote sensing of chemical agents. MacKerrow and Schmitt (1997) ran extensive experiments on speckle statistics from CO_2 LIDAR returns, while Nelson et al. (2000) used

(a) Sheen, DM. 2000. "Frequency modulation spectroscopy modeling for remote chemical detection." PNNL internal memo.

simulation techniques to study both turbulence and speckle for CO_2 LIDAR. Both of these studies were associated with the DOE CALIOPE project. Since FY00, the FM-DIAL system has used a retro-reflector for its target in lieu of a diffuse reflecting surface. This has enabled chemical detection experiments over path lengths of 10 km round-trip, but it has also removed speckle noise from the system, and has made atmospheric turbulence the dominant component of noise. Now that the turbulence problem has been studied, it is important to revisit the speckle problem and determine how the two noise sources compare over previously used path lengths of 2 km, 5 km, and 10 km round-trip.

4.1.1 Comparison of Speckle and Turbulence Noise on FM-DIAL

Over the past three years a large effort has been made to study the impact of turbulence on the FM-DIAL system and to mitigate those impacts. Field experiments of turbulence noise have been performed using lasers in both the SWIR and LWIR regimes over various path lengths. Monte-Carlo simulations have been run to compare against these results and to predict results for other wavelengths and path lengths.

To date a limited number of simulations have been run using a diffuse target in place of the retro-reflector. These simulations have been run in the absence of turbulence so that the signal-to-noise ratio (SNR) from the speckle noise could be measured for the system. Though the speckle simulation data set is incomplete at this time, it is illustrative to compare the SNR from the current speckle data set with the archived turbulence data set in order to gain an idea of the relative contributions of the two noise sources.

The speckle simulations used the same code as the turbulence simulations with the exception of the target surface's impact on the beam. There the electric field was randomized over the spatial domain via the equation

$$E_{reflected}(n_x, n_y) = E_{target}(n_x, n_y)\exp[2\pi i \times random(n_x, n_y)],$$

where random(n_x , n_y) is a random number between 0 and 1 selected from a uniform distribution. Here (n_x , n_y) denotes a pixel location. As well, the turbulence level was turned down so low that the noise contribution from turbulence scintillations would be negligible. Signal-to-noise results from 200 realizations per path length of 1 km, 2.5 km, and 4.8 km are shown in the table below.

It is reasonable to compare the turbulence data set against the speckle data set only if a value for C_n^2 is chosen that reflects average turbulence conditions. Experimental data suggests that C_n^2 = 1E-13 is an appropriate value. Pulling the data associated with this C_n^2 from the turbulence data set gives the compiled results shown in Table 4.1.

Table 4.1. Simulated Signal-to-Noise Ratio of Speckle and Turbulence-Induced Intensity Fluctuations Over Three Different Distances

Distance	Speckle Simulation SNR	Turbulence Simulation SNR
1 km	25.76	9.58
2.5 km	11.80	2.28
4.8 km	7.18	0.792

4.1.2 Limitations of the Current System with Regards to Speckle

The current FM-DIAL system is not well suited for the diffuse reflection of its laser beam off of target surfaces. The outgoing laser beam operates in continuous wave mode with an output power on the order of 5 mW though some devices have output powers approaching 100 mW. The beam's initial spot size radius of 3 mm also results in a large angular divergence of 1–2 mrad. The relative area of the transmitted beam to the target and the reflected beam to the telescope cause a large loss in return beam power. Lack of a retro-reflector in the system would exacerbate the power loss even further. For example, experiments were conducted in 2007 to determine how the reflection from several common targets over a 50-ft path length affected laser power albedo loss. A bike reflector caused a relative loss of 80% in the beam as compared with use of a retro-reflector. A license plate caused a 98% relative loss, while a cement block caused a 99.95% relative loss. Speckle noise would certainly dominate noise from turbulence over such a short path length, but return power loss is the biggest issue.

4.2 Addressing the Scale Problem in the Simulations

One of the biggest challenges with the numerical simulations is maintaining information on all the relevant scales. The initial laser spot size for the QCLs as well as the inner scale or smallest stable cell size for index of refraction fluctuations are both on the scale of millimeters. On the other hand, the 1–2 mrad divergence of the laser means that the laser spot is on the order of meters after propagating one kilometer. As a result, a complete simulation would require arrays with at least 4096×4096 elements. A single realization requires more than 90 two-dimensional Fourier transforms. A single realization using 512×512 arrays requires approximately 20 seconds to complete, whereas the time required for a single realization using 4096×4096 arrays is several minutes. In order to evaluate a single set of simulation parameters, a few thousand realizations should be run; as a result, one set of simulations using the 4096×4096 arrays would require one week of computational time. This quickly becomes impractical.

During the last part of FY07 we have been exploring other approaches for dealing with this problem. One possibility is keeping the number of array elements fixed (i.e., 512×512) but changing the resolution of each element. For example keeping a fixed array of 512×512 elements but in the near-field each element would be 1 mm in size and increase to a few cm in size in the far-field. The opposite technique could also be used, keeping the size of the elements the same but increasing the array size to encompass the beam. In this approach, the element size would stay fixed at 1 mm and the array size would start small in the near-field and become large in the far-field. Another approach would be introducing non-uniform phase screens. We have done some preliminary work in this area for introducing tip-tilt and beam wander effects into the simulations. Also, mode-coupling approaches to beam propagation in atmospheric turbulence have recently been reported by Schwartz and Dogariu (2006). Finally, all of these approaches are amenable to parallel computing, which can be taken advantage of to reduce the required computing time. Some preliminary research into these various approaches has taken place during FY07. We plan to continue this work in FY08.

5.0 Field Tests

Several field campaigns took place during FY07. In December, the broadband system had its first field deployment at the Hanford Town Site. Both the broadband and the SWIR FM-Mini systems were deployed at the HTS in June for the release of *Michigan*. In July, the broadband and LWIR FM-Mini systems detected the release of *New Hampshire* at the HTS. The last big field campaign of the year took place in August at the Nevada Test Site where both the broadband and LWIR FM-Mini systems were deployed during the *Tarantula* tests. The FM-Mini system will be deployed at the end of September to look at operation at up to 8-km distances. As these experiments have not taken place, the results will not be discussed here.

5.1 December Field Tests at the Hanford Town Site

The BLS was deployed at the HTS on December 20, 2006. These field tests were aimed at getting the first data from the broadband system in a stand-off configuration. In these experiments a 6-in. retro-reflector was placed 1.03 km from the trailer platform. Strong signals were returned at this range making data collection easy. Experiments were conducted throughout the morning and afternoon and conditions were overcast and cold, reducing the effects of turbulence as well as slowing the timescale of turbulence-induced intensity fluctuations.

Data was collected at a rate of 60 spectra per second, and organized into blocks (or sequences) of 50 spectra. A representative spectrum from the average of one sequence is shown in Figure 5.1. As can be seen from the time axis, the entire spectrum is recorded in 3.5 ms. The oscillations within the spectrum are due to the individual modes of the QCL, and are partially averaged out due to a small amount of timing jitter. The width of the spectrum shown is approximately 35 cm^{-1} from 1030–1065 cm^{-1}. For comparison, a typical narrowband QCL scans over approximately 1.5 cm^{-1}. The broadband emission will allow for the stand-off detection of chemical species with wider infrared absorption features on the order of 10–20 cm^{-1}.

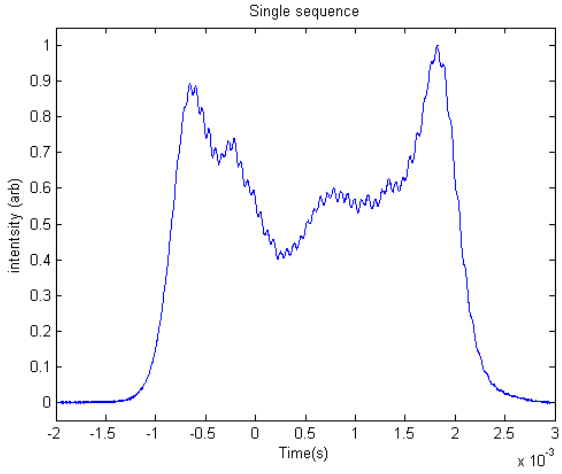

Figure 5.1. Representative Spectrum from the Average of One Sequence of 50 Spectra

The rate of data collection allowed some simple analysis of the turbulence conditions during the tests. Using autocorrelation, we were able to construct the turbulence timescale as shown in Figure 5.2. Because data was collected at 60 Hz, the shortest timescale that we can measure is 16.6 ms. We find that at this time scale, the return signals are 85% correlated. This is encouraging, as our data is collected on a faster timescale (3.5 ms) and will be strongly correlated (~97%) within a given spectrum. This has important ramifications for detection and indicates that turbulence will only cause the overall intensity of a recorded spectrum to fluctuate, and not induce excess turbulence noise within a single scan.

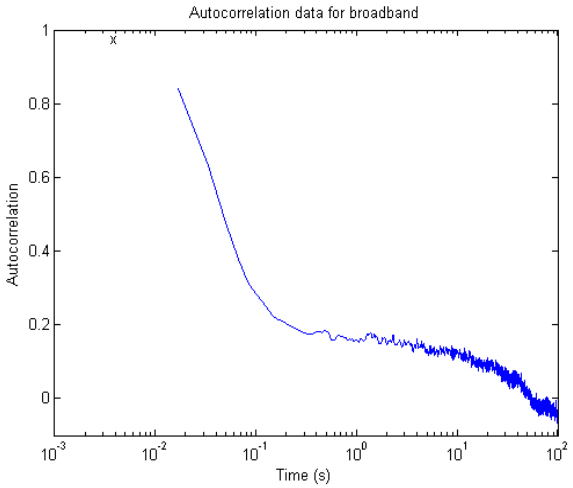

Figure 5.2. Autocorrelation Relation Plot Showing the Timescale of Atmospheric Turbulence

5.2 June *Michigan* Releases at the Hanford Test Site

One of our primary deliverables for the broadband task, as well as the primary project deliverable, was detecting atmospheric releases of *Michigan*. This chemical is a high-value signature of the nuclear proliferation process. This project has focused on trying to detect relevant chemicals for nuclear proliferation, and resist the temptation to use surrogate chemicals that are typically much easier to detect.

5.2.1 Experimental Setup

In order to release *Michigan*, we first had to develop a release apparatus capable of handling liquid samples. In the final design, we used our portable plume generator (PPG) that has been developed in previous years as the base. On the right-hand side of Figure 5.3, we see the PPG that consists of batteries, flow controllers, an RF receiver, and a nitrogen cylinder. The yellow light flashes to indicate when a release is taking place. The PPG was used to deliver a regulated amount of nitrogen flow to the *Michigan* bubbler that was temperature-regulated in a thermal bath. The thermal bath was placed in a catch basin to prevent any accidental spillage of *Michigan* or the recirculating temperature bath solution. The bubbler was housed within the temperature bath, and covered with insulation to stabilize the temperature. Approximately 1-liter samples of *Michigan* were loaded into the bubbler at a time. Output from the bubbler was taken to the release tube via heated stainless steel bellows tubing. Heating of this tube was

required to eliminate any condensation after the bubbler, which was at an elevated temperature. The release tube consisted of a blower mounted on the bottom of a 6-in. PVC tube where the *Michigan*/nitrogen flow was mixed with air. The resulting mixture was pushed out of the tube by the airflow from the blower.

Figure 5.3. Portable Plume Generator for *Michigan*

The *Michigan* release rate that we targeted was 1 g/s with fairly low airflows (35 cfm) out of the tube. For our experiments we try to use small quantities of chemicals and small plumes to minimize the amount of released chemicals and maximize the safety of our field tests. The bubbler was tested in a laboratory fume hood prior to use outside. We obtained mass release curves as a function of time for several different flow conditions and temperatures. The temperature and carrier gas flow rate was selected to give approximately 1 g/s *Michigan* release rates. Figure 5.4 shows the release apparatus as viewed from the same direction as the trailer location.

Figure 5.4. *Michigan* PPG as Viewed from the Trailer

A retro-reflector was deployed 1.01 km from the trailer near the tree at the end of the gravel road in Figure 5.4. The trailer deployment is shown in Figure 5.5, with the FM-Mini system deployed in front.

Figure 5.5. BLS Trailer and FM-Mini System Deployed for *Michigan* Release Experiments

We followed a strict procedure for the *Michigan* release that consisted of collecting background data before the release, initiating the release with an RF transmitter, collecting data for about 5 minutes, and then stopping the release apparatus. After stopping the release, the blower continues to run for another 2 minutes to make sure that any residual chemicals are purged from the release apparatus. We typically also collect background for 10 minutes after complete shutdown. We had a total of 10 release sequences, some consisting of multiple plume-on and plume-off subsequences.

The BLS and FM-Mini sensors both make column-integrated concentration measurements during which the laser must intersect the plume in order to have a positive detection. The wind was blowing at 20–30 miles per hour during many of the releases, causing the plume to break up rapidly and reducing the concentration. This made the measurements challenging; nevertheless, both the BLS and the FM-Mini detected *Michigan* during several release sequences.

5.2.2 FM-Mini Results

We encountered some difficulties with the data from the FM-Mini. The commercial SWIR laser used in the system was limited to modulation frequencies of 2 kHz. As a result the data had to be collected at a rate slower than the timescale of atmospheric turbulence fluctuations. This, combined with a phase jitter on the order of 1%, reduced the effectiveness of the intensity normalization techniques and significantly degraded the detection limits of the system. Spectral scans were collected in blocks of ten at 10 Hz. Each block was averaged and processed as a single trace. Background data was collected for approximately 10 minutes prior to releases and again for 5–10 minutes after releases were complete.

Figure 5.6 shows that the signal-to-noise using the SWIR components is not ideal, but a step function can be observed where the chemical was turned on and turned off.

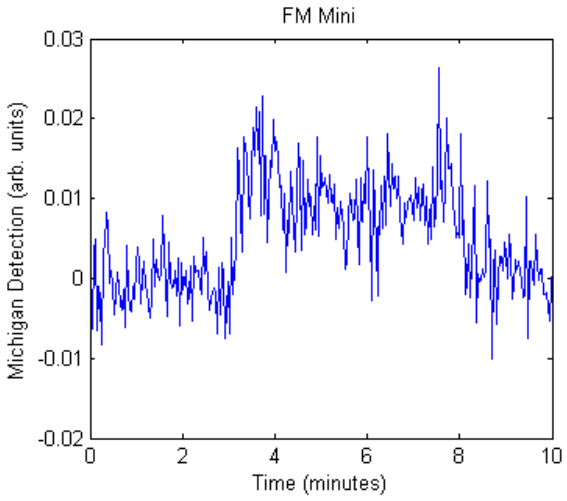

Figure 5.6. Processed FM-Mini Results for the *Michigan* Release Experiments

5.2.3 Broadband Results

The broadband system detected good signals on the first *Michigan* release. The data in Figure 5.7 is representative of what we collected during the field campaign. The upper panel shows a raw signal for a background trace in blue and a trace with *Michigan* absorption features green. The modes of the QC are partially resolved, and *Michigan* reduces the transmitted intensity of several modes at 1.1 ms, 1.4 ms, 1.8 ms, and 2.2 ms. Using the raw data traces, an absorption plot is shown in the blue trace on the bottom plot. The green trace represents the basis function that was used to fit the data. The four features seen in the absorption plot correspond to *Q*-branch features.

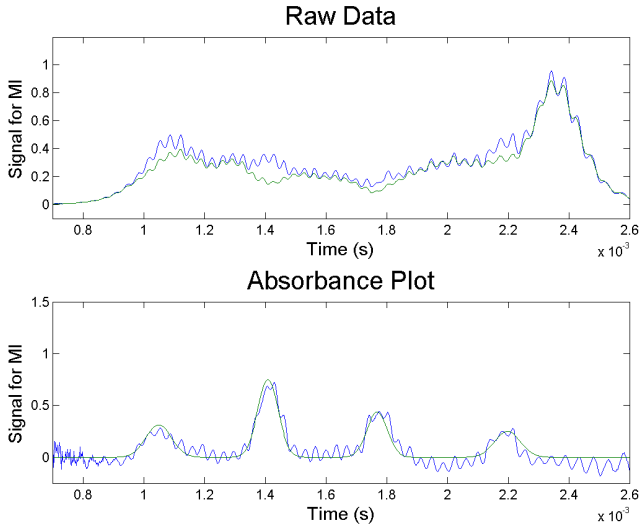

Figure 5.7. Representative Raw BLS Data for the *Michigan* Release Experiments

After acquiring many traces before, during, and after the release, our extended least squares fitting procedure was applied to the data. The results shown in Figure 5.8 clearly show the *Michigan* release occurring at 4 min and ending at 16 min. Subsequent releases had a similar quality of data.

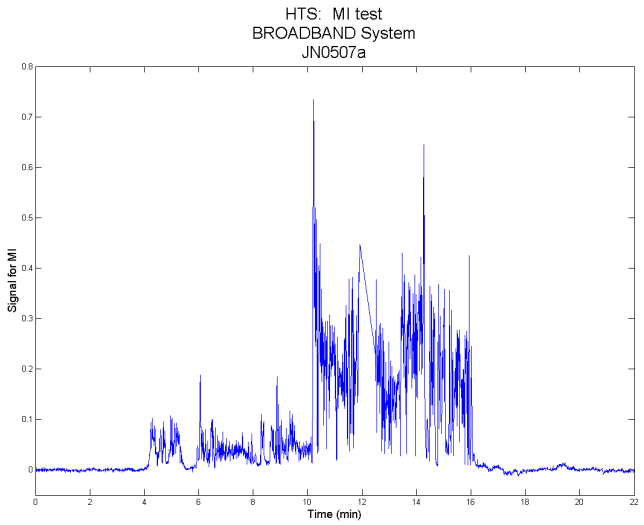

Figure 5.8. Processed BLS Results for the First *Michigan* Release

5.3 July *New Hampshire* Releases at the Hanford Town Site

In July 2007, both the FM-Mini and the BLS were reconfigured and deployed to detect *New Hampshire* during field tests at the Hanford Town Site. These tests helped prepare the team for the August *Tarantula* tests at the Nevada Test Site. The FM-Mini and BLS successfully detected *New Hampshire* during each of the releases.

5.3.1 Experimental Setup

The experimental setup of the release apparatus was similar to the *Michigan* releases, but simplified. No temperature bath was needed and the *New Hampshire* gas was seeded directly into the plume release tube via a flow controller. This type of release apparatus is similar to that used at NTS for chemical releases. Our release rate was about 0.06 kg/hr, or about 2% of the release rate of the NTS tests detailed below. This low release rate is consistent with our goal to operate close to the release point in order to maintain safety and a low-emission profile.

5.3.2 FM-Mini Results

The FM-Mini had much better results with the LWIR components detecting *New Hampshire*. This time the laser was modulated at 200 kHz, so atmospheric turbulence was less of a problem with the LWIR laser than with the SWIR laser. Spectral scans were collected at 20 Hz with 20 scans/sequence. The data was collected in a similar manner as previously with background data taken prior to and after releases.

Figure 5.9 shows the results obtained from the FM-Mini during the second release on July 17. The variability in the signal is driven by plume dynamics and changes in the wind speed and direction.

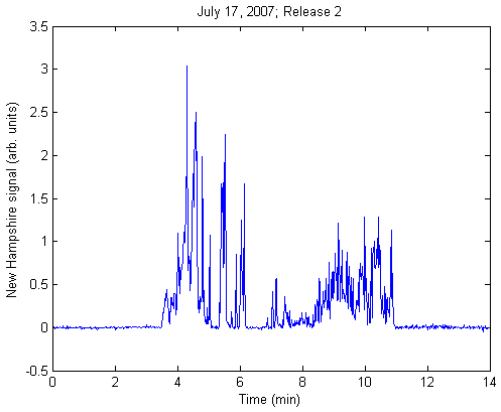

Figure 5.9. Processed FM-Mini Results for the Second *New Hampshire* Release

5.3.3 Broadband Results

A typical release scenario involves looking at background signals for several minutes before a release, monitoring a several-minute release, and then looking at backgrounds for the remaining time. We collected 125 spectra each second and averaged those into sequences of 50 for further processing. Some typical results are shown in Figure 5.10. Note the flat baseline before and after the 8-minute release. The significant fluctuations in the observed data are a result of mixing dynamics as the plume is leaving the release apparatus and traveling to the detection region. For faster winds we observed more intermittent signals. For more consistent and lower wind speeds, we observed a sustained signal, such as that shown in Figure 5.10. In this data there was a slight fade out in the middle, but the first and second part consistently generated a sustained signal. The fluctuations occur on the timescale of seconds and we have several data points across the faster fluctuations.

5.4 August *Tarantula* Tests at the Nevada Test Site

In August FY07, PNNL participated in the Brown Recluse process simulation conducted as part of the *Tarantula* tests at the Nevada Test Site. We were interested in using the BLS to detect *Michigan*; however, that chemical was not released as part of the simulation. Instead, we opted to use both the FM-Mini and the BLS to detect *New Hampshire*. Both sensors successfully detected the release of *New Hampshire*.

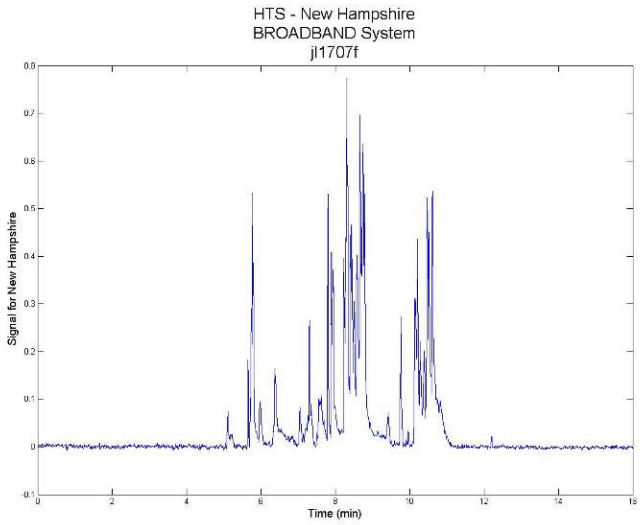

Figure 5.10. Processed BLS Results for the *New Hampshire* Release

5.4.1 Experimental Setup

On August 14, the remote sensing trailer left PNNL and made the trip to Mercury, Nevada. The FM-Mini system was transported within the trailer. The trailer arrived at NTS on August 15 and both sensors were deployed at Test Cell C (TCC) for chemical releases August 20–22. Three chemicals, including *New Hampshire*, were released using PPGs. The releases took place over a 3-hour period during the late morning/early afternoon of Monday, August 20, and Wednesday, August 22. Releases on Monday and Wednesday were similar, except for an upset during Wednesday's release. Figure 5.11 shows both the remote sensing trailer and the FM-Mini system deployed at TCC. The BLS trailer and FM-Mini systems are shown on the left, and the view of TCC as seen from the location of the sensors is shown on the right.

Figure 5.11. (left) BLS Trailer and FM-Mini System Deployed at NTS; (right) Test Cell C as Seen from the Sensor Locations

Electrical power was not available at TCC, so both sensors were powered by diesel generators. *New Hampshire* was released through a PPG located within the fence line of TCC. The BLS and FM-Mini were co-located approximately 500 m away from the release point. Two retro-reflector targets were placed so that the plume could be interrogated roughly 180 m and 270 m downwind of the release point. A schematic of the experimental setup is shown in Figure 5.12.

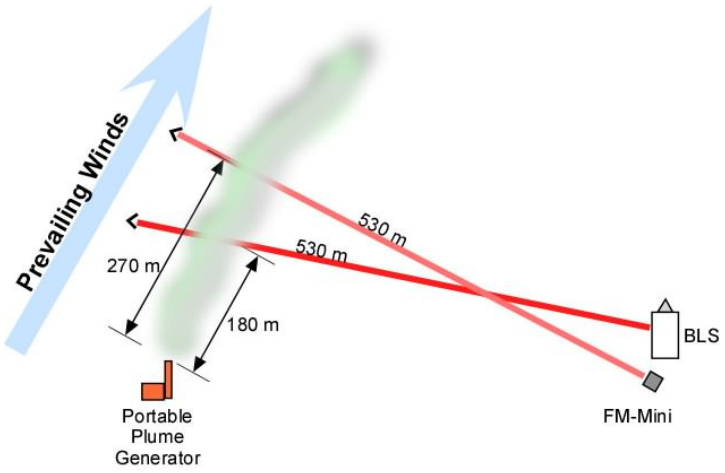

Figure 5.12. Schematic of the Experimental Setup at Test Cell C

Both sensors successfully detected and monitored the releases that took place on August 20, 2007. Prior to the start of the releases on August 22, the generator that was powering the BLS and FM-Mini failed. The sensors were not operational during the August 22 releases, and no data was collected.

5.4.2 FM-Mini Results

For this set of releases, the data acquisition was the same as that for the July *New Hampshire* releases at the Hanford Town Site. The results from the FM-Mini are shown in Figure 5.13. The plot on the left shows the data taken during the first half of the releases while the FM-Mini was interrogating the plume 180 m downwind from the release point. The first peak observed was a check of the release system to make sure that everything was operating properly. The data from 11.25 to 12.25 hours track well with the release rates provided by the Nevada Test Site. The release rates during the first half of the releases were considerably smaller than those during the second half, so the FM-Mini changed targets to interrogate the plume 270 m downwind of the release point during the last half of the releases. This data is shown on the right hand side of Figure 5.13.

The data around 12.6 hr was expanded to observe the mixing dynamics of the release apparatus. This is shown in Figure 5.14. From this plot, one can notice that the sampling rate is faster than the fluctuations due to the plume variations. These observations suggest that we could exploit this type of variation to optimize the degree of averaging and our sampling rates.

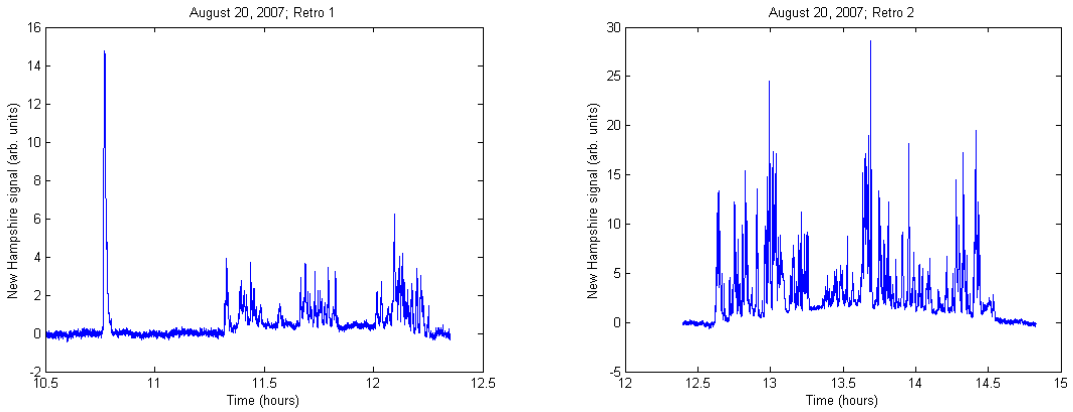

Figure 5.13. Processed *New Hampshire* Results of the FM-Mini System for the First (left) and Second (right) Halves of the August 20 Release

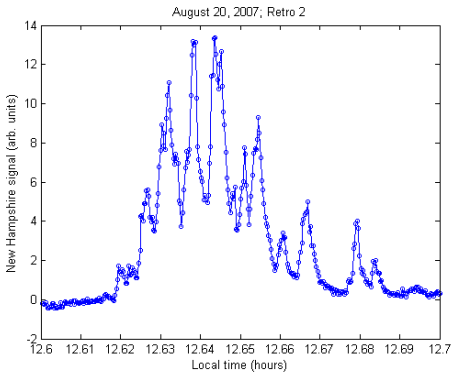

Figure 5.14. Blow Up of Data Collected Around 12:40 pm that Shows the Plume Dynamics

5.4.3 Broadband Results

We collected data in a similar manner as to the other tests that we performed this year. Broadband envelopes were collected at 125 spectra/second. Fifty spectra were accumulated, averaged, and then processed. These data were then fit with our extended least squares fitting procedure and the results are plotted in the Figure 5.15. The time axis is decimated time where 11.5 is equivalent to 11:30 am.

Our data tracks nicely with the release sequence schedule, where our data lags by about 2 minutes. Our laser beam path intersected the plume about 200 m downwind from the actual release point. When a release is initiated, based on the wind speeds, it took about 1–3 minutes for the plume to move to the interrogated path. We observed a similar time lag between the BLS data and the FM-Mini data when we probed two different beam paths during the second half of the release. Even 200 m from the release point, our signal-to-noise was quite good for positively detecting the chemical. Furthermore, these measurements give solid quantitative measurements about how much of *New Hampshire* crossed the beam path.

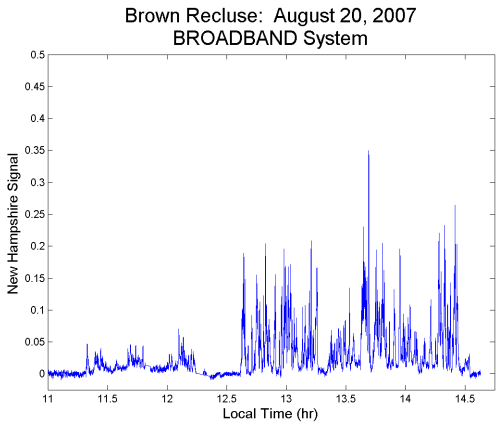

Figure 5.15. Processed *New Hampshire* Results for the August 20 Release

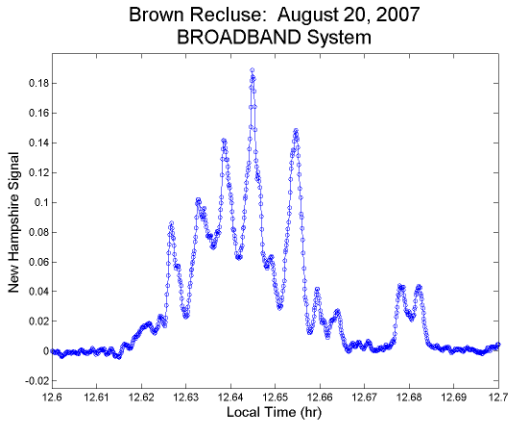

Figure 5.16. Blow Up of Data Collected Around 12:40 pm that Shows the Plume Dynamics

In addition to our sensor response, we also noted the mixing dynamics of the release apparatus. Figure 5.16 expands the above results of Figure 5.15 around 12.6 hr. Notice that the sampling rate (every 0.4s) is significantly faster than the fluctuations due to the plume variations which was observed to be on the 5–10 second timescale. These observations suggest that we could exploit this type of variation to optimize the degree of averaging and our sampling rates.

6.0 References

Abarbanel H, S Drell, N Fortson, J Goodman, S Koonin, N Lewis, G MacDonald, C Max, S Ride, S Sullivan and F Zachariasen. 1994. *Lidar*. JASON - The Mitre Corporation, McLean, Virginia.

MacKerrow EP and MJ Schmitt. 1997. "Measurement of integrated speckle statistics for CO_2 lidar returns from a moving, nonuniform, hard target." *Appl Optics* **36**(27):6921-6937.

Nelson DH, DL Walters, EP MacKerrow, MJ Schmitt, CR Quick, WM Porch and RR Petrin. 2000. "Wave Optics Simulation of Atmospheric Turbulence and Reflective Speckle Effects in CO_2 Lidar." *Appl Optics* **39**(12):1857-1871.

Schwartz C and A Dogariu. 2006. "Mode coupling approach to beam propagation in atmospheric turbulence." *J Opt Soc Am A* **23**:329-338.

Distribution

No. of Copies	No. of Copies

OFFSITE